



**HAL**  
open science

# Revisiting the mechanism of reversed thermoremanent magnetization based on observations from synthetic ferrian ilmenite ( $y = 0.7$ )

France Lacroix, Subir K. K. Banerjee, Bruce . M. Moskowitz

## ► To cite this version:

France Lacroix, Subir K. K. Banerjee, Bruce . M. Moskowitz. Revisiting the mechanism of reversed thermoremanent magnetization based on observations from synthetic ferrian ilmenite ( $y = 0.7$ ). *Journal of Geophysical Research: Solid Earth*, 2004, 109 (B12), pp.B12108. 10.1029/2004JB003076 . insu-01351587

**HAL Id: insu-01351587**

**<https://insu.hal.science/insu-01351587>**

Submitted on 4 Aug 2016

**HAL** is a multi-disciplinary open access archive for the deposit and dissemination of scientific research documents, whether they are published or not. The documents may come from teaching and research institutions in France or abroad, or from public or private research centers.

L'archive ouverte pluridisciplinaire **HAL**, est destinée au dépôt et à la diffusion de documents scientifiques de niveau recherche, publiés ou non, émanant des établissements d'enseignement et de recherche français ou étrangers, des laboratoires publics ou privés.

## Revisiting the mechanism of reversed thermoremanent magnetization based on observations from synthetic ferrian ilmenite ( $y = 0.7$ )

France Lagroix,<sup>1</sup> Subir K. Banerjee, and Bruce M. Moskowitz

Department of Geology and Geophysics, University of Minnesota, Minneapolis, Minnesota, USA

Received 10 March 2004; revised 16 August 2004; accepted 22 October 2004; published 28 December 2004.

[1] This study investigates the magnetic behavior of three well-characterized synthetic single-phase ferrian ilmenite ( $y = 0.7$ ) specimens over the temperature range between 10 K and 573 K. Careful experiments measuring induced and remanent magnetizations in variable temperatures, applied magnetic fields, and pretreatment conditions are conducted in order to elucidate the mechanism leading to reversed thermoremanent magnetization (RTRM). Magnetic ordering temperatures of the cation ordered domains, in all three samples, are estimated at 380 K, suggesting that their Curie temperatures ( $T_C$ ) are independent of the sample's thermal history. This is not the case for cation disordered boundaries resulting from quenching from high temperatures. These cation disordered domains have estimated magnetic ordering temperatures of 418 K (Q1300), 410 K (Q1050), and 425 K (Q900). The data unambiguously support a less than perfect ferrimagnetic–antiferromagnetic exchange interaction as the fundamental source of RTRM. Furthermore, the magnetic field strength of the “effective” exchange anisotropies in such polycrystalline samples are estimated at  $\sim 2.7$  mT (Q1300),  $\sim 12$  mT (Q1050), and 0 mT (Q900). However, from the results presented herein we conclude that favorable conditions for the acquisition of RTRM are dependent not only on the strength of the exchange anisotropy but also on the crucial role played by the size of the cation ordered domains. **INDEX TERMS:** 1519 Geomagnetism and Paleomagnetism: Magnetic mineralogy and petrology; 1540 Geomagnetism and Paleomagnetism: Rock and mineral magnetism; 1714 History of Geophysics: Geomagnetism and paleomagnetism; **KEYWORDS:** ferrian ilmenite, reversed thermoremanent magnetization, exchange anisotropy

**Citation:** Lagroix, F., S. K. Banerjee, and B. M. Moskowitz (2004), Revisiting the mechanism of reversed thermoremanent magnetization based on observations from synthetic ferrian ilmenite ( $y = 0.7$ ), *J. Geophys. Res.*, 109, B12108, doi:10.1029/2004JB003076.

### 1. Introduction

[2] The hematite–ilmenite solid solution series,  $y\text{FeTiO}_3 \cdot (1-y)\alpha\text{Fe}_2\text{O}_3$  ( $0 < y < 1$ ), has drawn much interest over the last 50 years due to the complexities of the chemical and magnetic properties arising from its significant dependence on thermal history. Both end-members have rhombohedral crystal structures and are antiferromagnetic below their magnetic ordering temperature (948 K for hematite and 63 K for ilmenite [Nagata and Akimoto, 1956]). However, the ilmenite crystal structure ( $R\bar{3}$ ) has a lower symmetry than that of hematite ( $R\bar{3}c$ ) owing to the higher degree of cation order in the ilmenite structure (i.e.,  $\text{Fe}^{2+}$  uniquely distributed within the A layer and  $\text{Ti}^{4+}$  within the B layer). A phase diagram (composition versus temperature) is shown in Figure 1 and displays both petrological and magnetic phase boundaries as compiled from numerous

studies [Ghiorso, 1997; Ishikawa *et al.*, 1985; Nagata and Akimoto, 1956; Nord and Lawson, 1989]. Herein we revisit the mechanism of reversed thermoremanent magnetization (RTRM), the phenomenon whereby a sample, upon cooling from above its Curie or Néel temperature ( $T_C$  or  $T_N$ ) in a magnetic field, acquires a TRM antiparallel to the applied field. Experimentally, through the analysis of synthetic samples, it has been determined that RTRM is a unique property of some single-phase ferrian ilmenite within the compositional range of  $0.51 < y < 0.73$  [Westcott-Lewis and Parry, 1971]. RTRM is also observed within a limited compositional range near the hematite end-member ( $0.15 < y < 0.25$ ) in slowly cooled phases displaying exsolution but in this case it is nonreproducible [Carmichael, 1961; Merrill and Grommé, 1967]. The mechanism leading to RTRM in each of the two compositional ranges differs, however, and the scope of this paper uniquely addresses the mechanism leading to RTRM in single-phase high titanium ferrian ilmenite.

[3] The first observation of RTRM was from a dacitic pumice ejected from the Haruna volcano in Japan [Nagata *et al.*, 1951], but the mineral phase acquiring the RTRM within the Haruna dacite was only identified a few years later [Nagata *et al.*, 1953]. In these early studies, the

<sup>1</sup>Now at Laboratoire de Paléomagnétisme, Institut de Physique du Globe de Paris, CNRS, Paris, France.

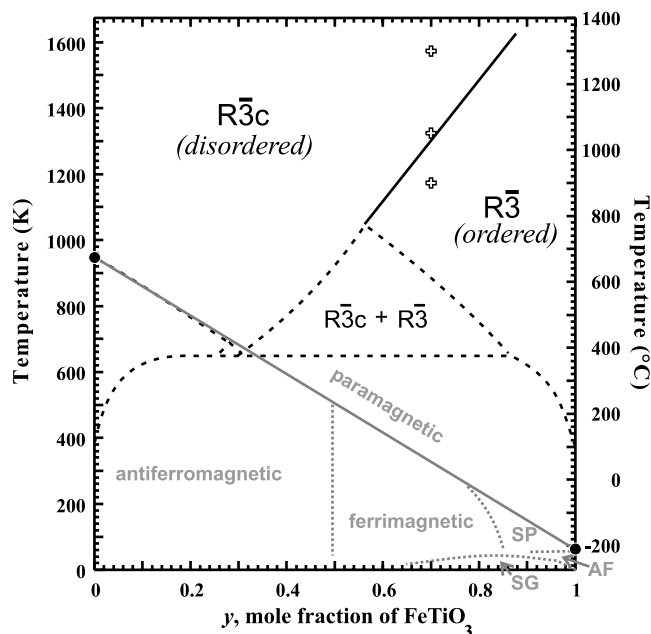


**Figure 1.** Phase diagram of composition versus temperature of the hematite-ilmenite solid solution series. End-member compositions, hematite ( $y = 0$ ) and ilmenite ( $y = 1$ ), are plotted as solid circles. Both petrological (black lines) and magnetic (gray lines) phase boundaries are plotted. Reversed thermoremanent magnetization in single-phase ferrian ilmenite is only observed when samples are quenched from above the cation order-disorder transition (solid black line, from Nord and Lawson [1989]). Dashed black lines, thermodynamic calculations by Ghiorso [1997], are phase boundaries associated with the solid solution's miscibility gap. Magnetic ordering temperatures (solid gray line) to a first approximation linearly decrease as  $y$  increases where  $T_C$  or  $T_N$  in  $^{\circ}\text{C} = 675 - 885y$  [Nagata and Akimoto, 1956]. However, slightly elevated ordering temperatures with respect to the linear trend are observed [Ishikawa, 1958] and are predicted by thermodynamic calculations [Ghiorso, 1997] in samples with greater cation order (i.e., higher  $y$  values). The other magnetic phase boundaries (dashed gray lines) are more uncertain and are the result of observations made by Ishikawa *et al.* [1985] (SP, superparamagnetic; SG, spin glass; AF, antiferromagnetic). The composition and quenching temperature of the synthetic samples investigated in this study are plotted as pluses.

mechanism for RTRM was speculated to result from the interaction between two phases where one phase (Ti poor titanomagnetite) had a higher  $T_C$  and lower spontaneous magnetization than the second phase (ferrian ilmenite). However, Uyeda [1955] determined that in fact both phases were compositions of the hematite-ilmenite solid solution series. Moreover, studies conducted on synthesized ferrian ilmenite samples of variable compositions and quenched from variable temperatures permitted the authors [Ishikawa and Akimoto, 1957; Uyeda, 1957, 1958] to establish that a systematic relationship exists between heat treatment, cation ordering and RTRM. This led to the determination of temperatures at which variable compositions undergo the transition from cation disorder to cation order [Ishikawa, 1958; Ishikawa and Syono, 1963; Nord and Lawson, 1989]

and the first observation by dark-field transmission electron microscopy of the coexistence of cation ordered and cation disordered regions within a single phase [Lawson *et al.*, 1981]. The role of magnetic exchange interaction in the origin of RTRM was speculated in the first proposed models of RTRM [Ishikawa, 1958; Uyeda, 1957]. However, it was the observation by Meiklejohn and Carter [1959, 1960], in synthetic samples of similar compositions to the Haruna dacite, of hysteresis loops shifted in the positive field direction by 35 mT after being cooled from above their  $T_C$  in a magnetic field that unambiguously confirmed the role of exchange anisotropy in the origin of RTRM.

[4] Since the earlier models of Uyeda [1958] and Ishikawa [1958], several hypotheses for the origin of RTRM have been proposed. Common to all hypotheses are the following observations: (1) Only single-phase ferrian ilmenite quenched at temperatures above that of the cation order-disorder transition may develop a RTRM. (2) The cation distribution within the single-phase ferrian ilmenite is heterogeneous, where some regions have a greater cation ordering than others. (4) The Fe content and the magnetic ordering temperature is inversely proportional to the degree of cation order (i.e., cation ordered regions have lower Fe content and hence a lower  $T_C$  than more disordered regions). (5) Cation order leads to ferrimagnetism, while cation disorder leads to antiferromagnetism with a small parasitic moment. (6) Cation ordered regions (region 1) acquire the RTRM. (7) RTRM results from an exchange anisotropy between region 1 and region 2 where cation layers (A and B) at the interface between regions 1 and 2 are in antiphase and region 2 is more Fe-rich and magnetically orders at a temperature higher than region 1.

[5] The main contrast between the various proposed models for the origin of RTRM is the nature of the magnetic order of region 2. Do RTRMs result from exchange anisotropy between region 1 and a second ferrimagnetic cation ordered domain, Ishikawa's "x phase" [Ishikawa, 1958; Ishikawa and Syono, 1963; Prévot *et al.*, 2001] or is region 2 cation disordered and antiferromagnetic [Hoffman, 1975; Nord and Lawson, 1992; Uyeda, 1958]? The goal of this study is to attempt to elucidate the nature of the magnetic order of region 2 by conducting magnetic experiments on synthetic ferrian ilmenites ( $y = 0.7$ ) over the temperature range of 10 K to 573 K. Furthermore, the three synthetic samples quenched from different temperatures, and analyzed and described in the following section, permitted us to investigate the consequences of the size of cation ordered domains on the acquisition of RTRM. The size of the cation ordered domains has been previously considered as a possible controlling factor in the origin of RTRM [Bina *et al.*, 1999; Goguitchaichvili and Prévot, 2000; Westcott-Lewis and Parry, 1971].

## 2. Description of the Synthetic Samples

[6] The synthetic ferrian ilmenite ( $y = 0.7$ ), referred herein as  $\text{Ilm}_{70}\text{Hem}_{30}$  samples, analyzed in this study were synthesized by C.A. Lawson. In studies published by C. A. Lawson and his colleagues the three  $\text{Ilm}_{70}\text{Hem}_{30}$  synthetic samples differing in thermal histories are labeled 70 01 00, 70 23 00 and 70 02B 01. All samples were synthesized from sintered pellets of a mixture of  $\text{Fe}_2\text{O}_3$  and  $\text{TiO}_2$  held

**Table 1.** A List of Certain Parameters Measured by *Nord and Lawson* [1989, 1992] Characterizing the Three Synthetic Samples Investigated in This Study

Sample Name							Surface Area Per Unit Volume of Cation Disordered Regions, $\times 10^{-6} \text{ m}^2/\text{m}^3$	Average Size of Cation Ordered Domains, $\mu\text{m}$
This Study	<i>Nord and Lawson</i> [1989, 1992]	Annealing Time, hours	Quenching Temperature, $^{\circ}\text{C}$ , K	Room Temperature $M_s$ , <sup>a</sup> $\text{Am}^2/\text{kg}$	$T_{\text{UB}}$ , <sup>b</sup> K	$T_B$ , <sup>b</sup> K		
Q1300	700100	0	1300, 1573	$30.1 \pm 0.7$	407	421	28.3	$0.071 \pm 0.005^c$
Q1050	702300	10	1050, 1323	$26.1 \pm 0.4$	397	407	54.5	$0.037 \pm 0.005$
Q900	7002B01	100	900, 1173	$36.0 \pm 0.3$	415	419	0.06	$\sim 35$

<sup>a</sup>Room temperature  $M_s$  was calculated by extrapolating to infinite magnetic fields induced moments measured in magnetic fields ranging from 0.3 to 0.75 T.

<sup>b</sup> $T_{\text{UB}}$  and  $T_B$  were determined from  $M_{[0.5T]}$  versus temperature heating and cooling curves respectively. *Nord and Lawson* [1989, 1992] refer to these as  $T_C$ . See section 3 for further explanation.

<sup>c</sup>This value was determined on a different sample (700200 from *Nord and Lawson* [1989]) that underwent the same synthesis and thermal history.

at  $1300^{\circ}\text{C}$  for a minimum of 36 hours in a furnace outfitted with a flowing gas mixture maintaining an oxygen fugacity of  $-5.68$  [*Lawson*, 1981]. Sample 70 01 00 was then quenched from  $1300^{\circ}\text{C}$  by being dropped in liquid nitrogen [*Lawson et al.*, 1981; *Nord and Lawson*, 1992]. Sample 70 23 00 was subsequently annealed at  $1050^{\circ}\text{C}$  for 10 hours before being quenched [*Nord and Lawson*, 1989, 1992]. Finally, sample 70 02B 01 was annealed at  $900^{\circ}\text{C}$  for 100 hours before being quenched [*Lawson et al.*, 1981; *Nord and Lawson*, 1989; *Nord and Lawson*, 1992]. The three specimens studied here have never been heated after being synthesized. For the sake of simplicity and clarity, hereafter we will refer to the specimen of sample 70 01 00 as Q1300, of sample 70 23 00 as Q1050, and of sample 70 02B 01 as Q900, denoting the  $\text{Ilm}_{70}\text{Hem}_{30}$  sample's final quenching (Q) temperature in degrees Celsius. Therefore Q1300 and Q1050 were quenched from a temperature higher than that of the cation order-disorder transition, while Q900 was quenched from a temperature below that of the cation order-disorder transition (see Figure 1). The single-phase nature of these samples has been assessed through reflected light, scanning electron and transmission electron microscopy techniques as well as electron microprobe analyses [*Lawson*, 1981; *Nord and Lawson*, 1989]. Of the three samples under consideration in this paper all were identified as being a single-phase  $\text{Ilm}_{70}\text{Hem}_{30}$ , however a titanomagnetite ( $\sim 50$  mol % ulvöspinel) phase was identified within Q1050. *Nord and Lawson* [1992] stated that this phase does "not appear to affect the magnetic properties. . . except the thermal demagnetization of TRM." In our experiments while the overall effect due to the presence of the titanomagnetite phase is negligible, as *Nord and Lawson* [1992] assessed, its presence is frequently observable. A compilation of results obtained in previous studies [*Lawson*, 1981; *Nord and Lawson*, 1989, 1992] concerning the three samples studied here are listed in Table 1. The key features distinguishing the three samples are the ratio of cation ordered regions to cation disordered regions and the size of the cation ordered domains. Q900 displays nearly complete cation order and consequently contains very large, on average  $\sim 35 \mu\text{m}$ , cation ordered domains. Q1300 and Q1050, quenched from above the cation order-disorder transition, have much smaller cation ordered domains, on average  $\sim 70$  nm and  $40$  nm respectively. Furthermore, Q1050

contains twice as much cation disordered regions than Q1300. The grain size of the synthetic samples range, overall, between 20 and  $300 \mu\text{m}$  [*Nord and Lawson*, 1992].

[7] In the following two sections, we present results and interpretations of experiments which led to the determination of magnetic ordering temperatures (section 3) and estimation of the effective exchange anisotropy strength (section 4). These are presented and discussed independently and at the forefront because together they provided the parameters justifying the setup of the remanence experiments presented in section 5.

### 3. Magnetic Ordering Temperature Determination

[8] The experiments and results presented in this section aimed, in part, to verify that the specimens had not suffered alterations during the time elapsed since their synthesis in the early 1980s. Furthermore, the maximum fields available and applied in the studies by *Nord and Lawson* [1989, 1992] to determine the magnetic ordering temperatures were quite low ( $0.5\text{T}$ ) such that magnetic saturation was probably not achieved. Table 2 of *Nord and Lawson* [1992] lists Curie temperatures ( $T_C$ ) upon warming and upon cooling. Given the unsaturated state of the samples due to the low magnetic fields applied ( $0.5\text{T}$ ) their magnetic ordering temperatures are more accurately magnetic unblocking temperatures ( $T_{\text{UB}}$ ) on warming and magnetic blocking temperatures ( $T_B$ ) on cooling. Therefore, in our Table 1 we list their magnetic ordering temperatures as  $T_{\text{UB}}$  and  $T_B$  even though in the original publication they are referred to as  $T_C$ .

[9] We measured the temperature dependence of high field induced moments and hysteresis loops using a vibrating sample magnetometer (VSM, Princeton Measurements), equipped with a helium cryostat for the 10 to 400 K temperature range or equipped with a flowing helium gas furnace for the 300 to 573 K temperature range (data shown in Figure 2). At room temperature (i.e., 300 K) our measured  $M_s$  in 1.5 T using the low-temperature VSM are  $31.2 \text{ Am}^2/\text{kg}$ ,  $26.9 \text{ Am}^2/\text{kg}$ , and  $34.9 \text{ Am}^2/\text{kg}$  for Q1300, Q1050 and Q900 respectively. These values are very close to values extrapolated to infinite fields calculated by *Nord and Lawson* [1992] listed in Table 1. Given that the specimens have undergone no experiments and no heat

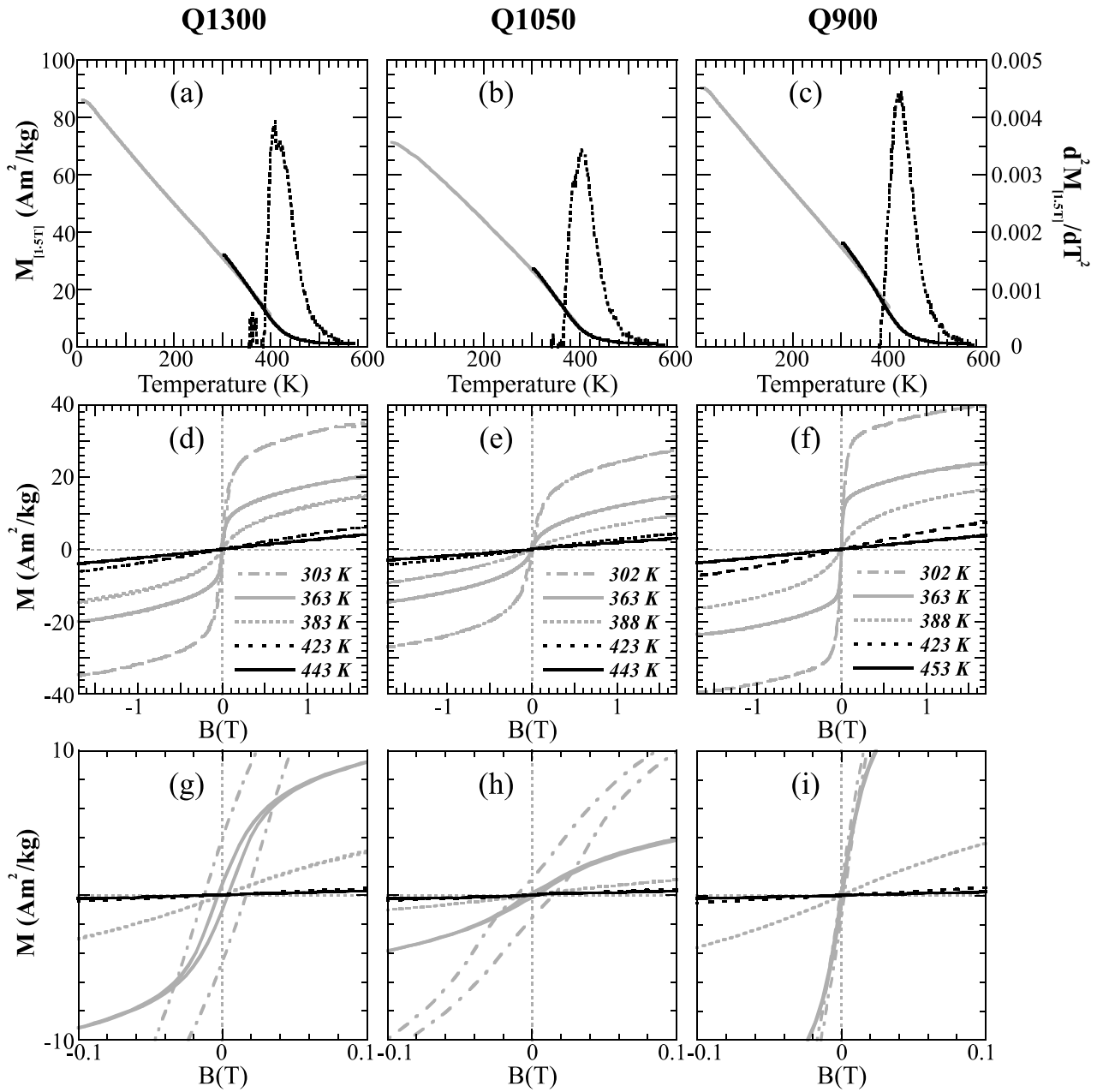


**Figure 2.** Induced magnetization in a 1.5 T magnetic field across the 10 K to 573 K temperature range measured on a VSM equipped with a helium cryostat (gray line) and a flowing helium gas furnace (solid black line) for (a) Q1300, (b) Q1050, and (c) Q900. The magnetic ordering temperature of the cation disordered boundaries was calculated from the second derivative of the high-temperature  $M_{[1.5T]}$  data (dashed black line) and results are listed in Table 3. Hysteresis loops measured across variable temperatures in the vicinity of the magnetic ordering temperature for (d) Q1300, (e) Q1050, and (f) Q900. (g–i) Details at the origin of the same hysteresis loops displayed in Figures 2d–2f. Hysteresis loop parameters are listed in Table 2 along with data at temperatures not plotted.

treatments since their synthesis, these results provide assurance that the specimens have not suffered from chemical alteration.

[10] The high sloped linear decrease of  $M_S$  with increasing temperature observed in our data (Figures 2a–2c) appears characteristic of ferrimagnetic samples exhibiting ferrimagnetism, as initially observed by *Ishikawa and Akimoto* [1957]. The  $M_S(T)$  segment measured on the high

temperature VSM was measured in 1.5 T and 1.7 T upon heating and cooling. Only the heating curves in 1.5 T are shown in Figures 2a–2c. Curves were reversible for Q1300 while for Q1050 and Q900  $M_S$  on cooling was slightly lower than on heating. Hysteresis loop parameters ( $M_R$ ,  $M_S$  and  $B_C$  are shown in Table 2) measured prior to and following the  $M_S(T)$  experiment suggest the slight irreversibility seen in Q1050 and Q900 is most likely not the result

**Table 2.** Hysteresis Loop Parameters at Variable High Temperatures

Sample	Mass, $\times 10^{-6}$ kg	Temperature, K	$M_S, \times 10^{-6}$ Am <sup>2</sup>	$M_S, \text{Am}^2/\text{kg}$	$M_R, \times 10^{-6}$ Am <sup>2</sup>	$M_R, \text{Am}^2/\text{kg}$	$B_C, \text{mT}$
Q1300	21.12 ± 0.10	300 <sup>b</sup>	724.9	34.32 ± 0.16	83.90	3.973 ± 0.019	13.7
Q1300	21.12 ± 0.10	303 <sup>c</sup>	733.7	34.74 ± 0.16	90.15	4.268 ± 0.020	14.6
Q1300	21.12 ± 0.10	299 <sup>d</sup>	705.6	33.41 ± 0.16	88.32	4.182 ± 0.020	15.6
Q1300	21.12 ± 0.10	334	531.0	25.14 ± 0.12	66.87	3.166 ± 0.015	11.1
Q1300	21.12 ± 0.10	363	423.9	20.07 ± 0.10	18.78	0.889 ± 0.004	3.54
Q1300	21.12 ± 0.10	383	311.9	14.77 ± 0.07	0.718	0.034 ± 0.000	0.95
Q1300	21.12 ± 0.10	403	207.7	9.83 ± 0.05	0.445	0.021 ± 0.000	2.94
Q1300	21.12 ± 0.10	423	131.3	6.22 ± 0.03	0.171	0.008 ± 0.000	1.52
Q1300	21.12 ± 0.10	443	84.81	4.02 ± 0.02	0.103	0.005 ± 0.000	0.97
Q1050	30.70 ± 0.11	300 <sup>b</sup>	872.9	28.43 ± 0.10	44.28	1.442 ± 0.005	11.9
Q1050	30.70 ± 0.11	302 <sup>c</sup>	833.3	27.14 ± 0.10	42.00	1.368 ± 0.005	12.6
Q1050	30.70 ± 0.11	300 <sup>d</sup>	841.5	27.41 ± 0.10	43.78	1.426 ± 0.005	13.1
Q1050	30.70 ± 0.11	363	448.4	14.61 ± 0.05	4.837	0.158 ± 0.001	2.89
Q1050	30.70 ± 0.11	388	285.6	9.30 ± 0.03	1.255	0.041 ± 0.000	2.34
Q1050	30.70 ± 0.11	423	133.1	4.34 ± 0.02	0.777	0.025 ± 0.000	3.21
Q1050	30.70 ± 0.11	433	108.5	3.53 ± 0.01	0.752	0.024 ± 0.000	2.83
Q1050	30.70 ± 0.11	443	91.84	2.99 ± 0.01	0.508	0.017 ± 0.000	1.94
Q1050	30.70 ± 0.11	473	61.12	1.99 ± 0.01	0.571	0.019 ± 0.000	2.65
Q1050	30.70 ± 0.11	523	40.20	1.31 ± 0.00	0.160	0.005 ± 0.000	1.48
Q900	17.14 ± 0.11	298 <sup>b</sup>	713.5	41.63 ± 0.27	18.55	1.082 ± 0.007	1.43
Q900	17.14 ± 0.11	302 <sup>c</sup>	676.9	39.49 ± 0.25	18.28	1.067 ± 0.007	1.43
Q900	17.14 ± 0.11	298 <sup>d</sup>	643.7	37.56 ± 0.24	15.63	0.912 ± 0.006	1.62
Q900	17.14 ± 0.11	363	403.9	23.56 ± 0.15	6.542	0.382 ± 0.002	0.55
Q900	17.14 ± 0.11	388	281.6	16.43 ± 0.11	0.246	0.014 ± 0.000	0.29
Q900	17.14 ± 0.11	423	127.3	7.43 ± 0.05	0.135	0.008 ± 0.000	0.98
Q900	17.14 ± 0.11	453	0.647	0.04 ± 0.00	0.234	0.014 ± 0.000	3.41
Q900	17.14 ± 0.11	473	0.459	0.03 ± 0.00	0.000	0.000 ± 0.000	-

<sup>a</sup>Because of the mounting process, the mass of the samples measured on the high-temperature VSM is unknown but was calculated from the 100 K temperature overlap of the high- and low-temperature  $M_{[1.5T]}$  data (see Figures 2a–2c), where the mass of samples for the low-temperature measurements is known.

<sup>b</sup>These values were measured prior to any heating.

<sup>c</sup>These values were measured following heating and cooling for  $M_S(T)$  experiment shown in Figures 2a–2c.

<sup>d</sup>These values were measured following heating and cooling for hysteresis loop versus temperature experiment included in Table 2 and shown in Figures 2d–2i and before  $B_{CR}$  versus temperature experiment shown in Figure 9 and for data listed in Table 4.

of chemical alterations. The most compelling evidence is the little to no change observed in  $B_C$ .

[11] We determined the ordering temperature by calculating the second derivative of the  $M_S(T)$  data measured at 1°C intervals on the high-temperature VSM. The temperature at which  $d^2M/dT^2$  reaches a maximum coincides with the inflection point and hence with the estimated  $T_C$  [Tauxe, 1998]. This method was applied previously [Lagroix *et al.*, 2004] where multiple mineral phases did not permit the use of more traditional methods [Ade-Hall *et al.*, 1965; Grommé *et al.*, 1969; Moskowitz, 1981]. Even though, in this study, we do not have multiple mineral phases, we feel this method produces an accurate determination of the inflection point of the  $M_S(T)$  curve which is the sought after temperature when applying the graphical method [Grommé *et al.*, 1969]. For comparison, listed in Table 3 are the magnetic ordering temperatures determined using the second derivative method and the graphical method.  $M_S(T)$  data determine in fields of 1.5 T and 1.7 T both yielded the same  $T_C$ . On the basis of the magnetic ordering phase boundary drawn in Figure 1 from the equation of Nagata and Akimoto [1956] (see caption of Figure 1)  $T_C$  for  $\text{Ilm}_{70}\text{Hem}_{30}$  should be 328 K. Our estimated  $T_C$  is 418 K for Q1300, 410 K for Q1050 and 425 K for Q900. These values are, respectively, 90 K, 82 K and 97 K higher than this predicted value based on the work of Nagata and Akimoto [1956]. However, on the basis of more recent thermodynamic analyses by Ghiroso [1997]  $T_C$  for  $\text{Ilm}_{70}\text{Hem}_{30}$  with high cation ordered is estimated at  $\sim 390$  K. This temperature is still lower than our measured values but only by 20 to 35 K.

[12] The hysteresis loops shown in Figures 2d–2i are linear above the determined  $T_C$ , with the exception of sample Q1050 which displays some hysteresis at the origin persistently to temperatures well above the determined  $T_C$  (highest temperature measured was 523 K). Moreover,  $M_S(T)$  data at low temperatures for this same sample (Figure 2b) show some curvature, in contrast to the other two samples (Figures 2a and 2c). Both of these features, persistence of hysteresis at high temperatures and nonlinearity of  $M_S(T)$  data, result from the presence of the small amounts of titanomagnetite identified by Nord and Lawson [1992] and mentioned above in section 2. For all samples in Figures 2c–2f (and expanded view in Figures 2g–2i), the well-defined shoulder of the hysteresis loops at 303 K and 363 K is significantly suppressed in the hysteresis loop at 383 K and at temperatures above resulting from a drastic loss of remanent magnetization (see Table 2). Low-field AC magnetic susceptibility measurements (Figure 3a) also dis-

**Table 3.** Estimation of  $T_C$  Determined by the Graphical Method Compared to That Calculated From the Second Derivative of  $M_S(T)$  Data<sup>a</sup>

Sample Name	Graphical Method, K	$d^2M/dT^2$ , K
Q1300	432	418
Q1050	415	410
Q900	435	425

<sup>a</sup>For the graphical method, see Grommé *et al.* [1969].

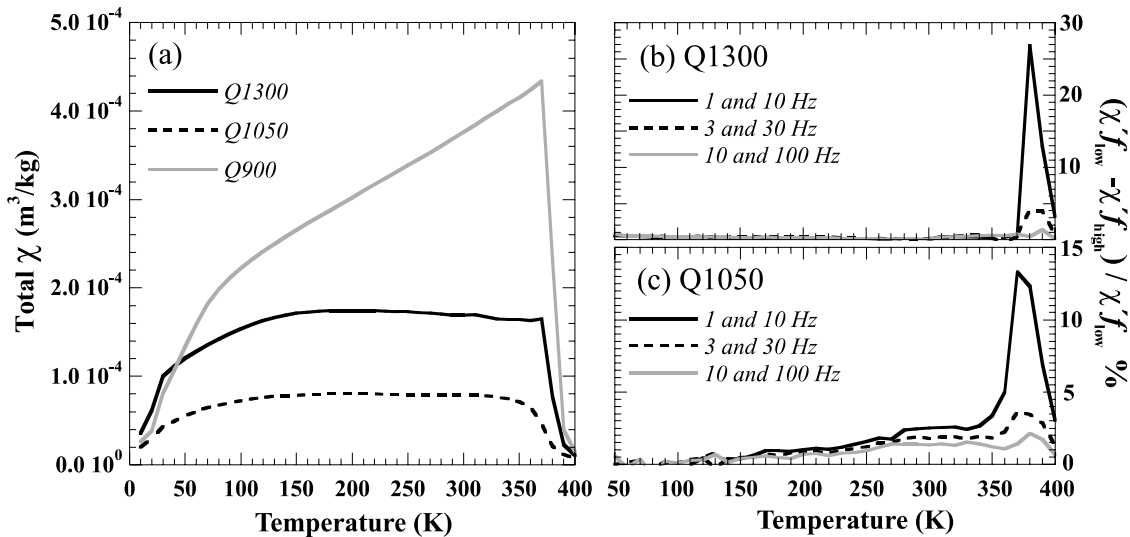


**Figure 3.** (a) Magnetic susceptibility (Total  $\chi$ ) measured in an AC field with peak amplitude of 80 A/m and a frequency of 1 Hz using the magnetic properties measurement system (MPMS; Quantum Designs). Total  $\chi$  equals  $\sqrt{(\chi'{}^2 + \chi''{}^2)}$ , where  $\chi'$  and  $\chi''$  are the in-phase and quadrature components of the AC magnetic susceptibility. Frequency dependence of the in-phase magnetic susceptibility ( $\chi'$ ) for (b) Q1300 and (c) Q1050.

play a substantial increase in induced magnetization upon cooling between 390 K and 370 K. This observation, coupled with the hysteresis measurements across this temperature range, indicates that the cation ordered region (i.e., ferrimagnetic region 1) magnetically orders at approximately 380 K. Such an ordering temperature for the cation ordered domains is in close agreement with a  $T_C$  of 390 K calculated by thermodynamic analysis [Ghiorso, 1997]. Consequently, the  $T_C$  observed at higher temperatures (418 K for Q1300, 410 K for Q1050 and 425 K for Q900) are associated with region 2 which we argue is the antiferromagnetic cation disordered boundary and the data presented herein support such a conclusion.

#### 4. Exchange Anisotropy: Estimating Its Effective Strength

[13] We qualify the strength of the exchange anisotropy by “effective” signifying the fact that in a polycrystalline sample we can not hope to observe the “true” exchange coupling present between one ferrimagnetic and one, say, antiferromagnetic crystal. Additionally, even in a single crystal the observed exchange anisotropy is the average of many contact surfaces and interfacial roughness between the two phases. From the dark-field microscopy images shown by Lawson *et al.* [1981] and Nord and Lawson [1992], one observes that the intricate patterns formed by the cation ordered domains and the cation disordered boundaries are similar in all samples quenched at a temperature exceeding that of the cation order-disorder transition. However, these images predominantly differ in the size and shape of the cation ordered domains which do not have equal dimensions within a sample. The similarity of patterns between samples quenched at different temperatures led us to believe that the distribution of the cation ordered domain sizes and shapes between samples is unique, differing only in the

mean cation ordered domain size. Consequently, surface area of contact between cation ordered and disordered regions, which is highly dependent on the size and shape of the cation ordered domains, should vary coherently with the mean size of the cation ordered domains within a polycrystalline sample. Logically, the surface area of contact is inversely proportional to the size of the cation ordered domains.

[14] The effective strength of the exchange anisotropy coupling the magnetic moments of the cation ordered domains antiferromagnetically to the magnetic moments of region 2 may be assessed from the behavior of the sample’s hysteresis loop measured following a field-cooling (FC) pretreatment relative to that following a zero-field cooling (ZFC) pretreatment [Meiklejohn, 1962; Meiklejohn and Bean, 1957]. We conducted such an experiment on all three specimens using a magnetic properties measurement system (MPMS, Quantum Designs). The samples were ZFC from 400 K to 150 K where a hysteresis loop with a maximum field of 2.5 T was measured. The sample was returned to 400 K in zero field before being field-cooled in 2.5 T to 150 K where the FC hysteresis loop was measured. In maximum fields of 2.5 T, the hysteresis loops are major loops. The observed additional increase in  $M_S$  with increasing fields, after the loop closes, results from the antiferromagnetic parasitic moment. At 400 K, we are above the ordering temperature of the cation ordered domains, a necessary experimental condition in order to assess the strength of the exchange anisotropy resulting in a RTRM in the cation ordered domains. The experiment was set up so as to have the cooling field direction parallel to the positive field direction during the hysteresis measurement. We expect to observe positive exchange bias characterized by FC loops shifted with respect to ZFC loops in the positive field direction. This shift would result from a preemptive reversal of the ferrimagnetic moment due to the antiferro-

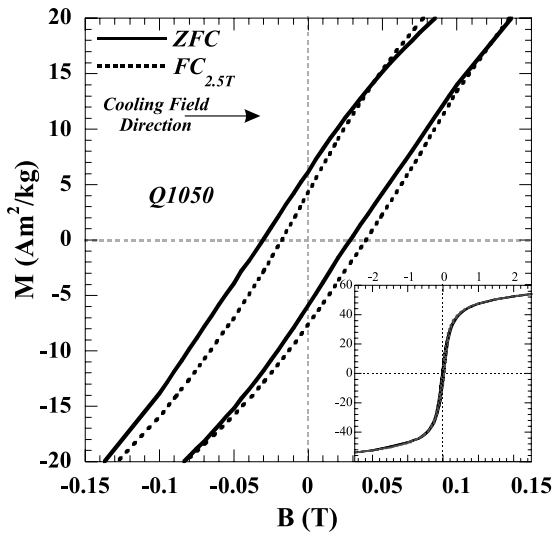


**Figure 4.** Hysteresis loops of Q1050 measured at 150 K following a zero-field cooling (ZFC) pretreatment from 400 K to 150 K and a 2.5 T field cooling (FC) pretreatment from 400 K to 150 K. Inset shows the complete ZFC and FC hysteresis loops, while the main plot displays an approximate 12 mT shift in the cooling field direction of the FC hysteresis loop with respect to the ZFC hysteresis loop. See section 4 for further explanation.

magnetic exchange interaction with the cation disorder boundaries prior to the actual magnetic field reversal during the measurement of the descending branch of the hysteresis loop. Conversely, while measuring the ascending branch of the hysteresis loop the exchange anisotropy will delay the flipping of the ferrimagnetic moment until the magnetic field has achieved a certain magnitude in the positive field direction.

[15] Plotted in Figure 4 are the ZFC and FC hysteresis loops for sample Q1050. The descending and ascending branches of the FC loop are shifted in the cooling field direction (positive exchange bias) by 13.84 mT and 10.39 mT respectively relative to the ZFC loop. We estimate that the exchange anisotropy of Q1050 is approximately 12 mT (average of the two values). Similarly, we determined that the effective exchange anisotropy of sample Q1300 is approximately 2.7 mT, where the descending and ascending branches of the FC loop are shifted in the cooling field direction by 5.01 mT and 0.40 mT respectively relative to the ZFC loop (not shown). No shift between ZFC and FC hysteresis loops was observed for sample Q900. Because Q900 was quenched at a temperature below the cation order-disorder transition it can not acquire a RTRM, and therefore no shifting of FC loops with respect to ZFC loops was expected.

## 5. Remanent Magnetization Experiments

[16] The following sections will present results from several remanent magnetization experiments. The interpretation of these results will be discussed in Section 6. While many interesting features are observed at very low temperature (i.e., below 100 K) they are beyond the scope of this

paper. Special attention in future research will be placed on these phenomena in order to understand such complex behavior observed in titanium rich phases of the hematite-ilmenite solid solution series at very low temperatures where spin glass and spin cluster behaviors may be expected [e.g., *Ishikawa et al.*, 1985].

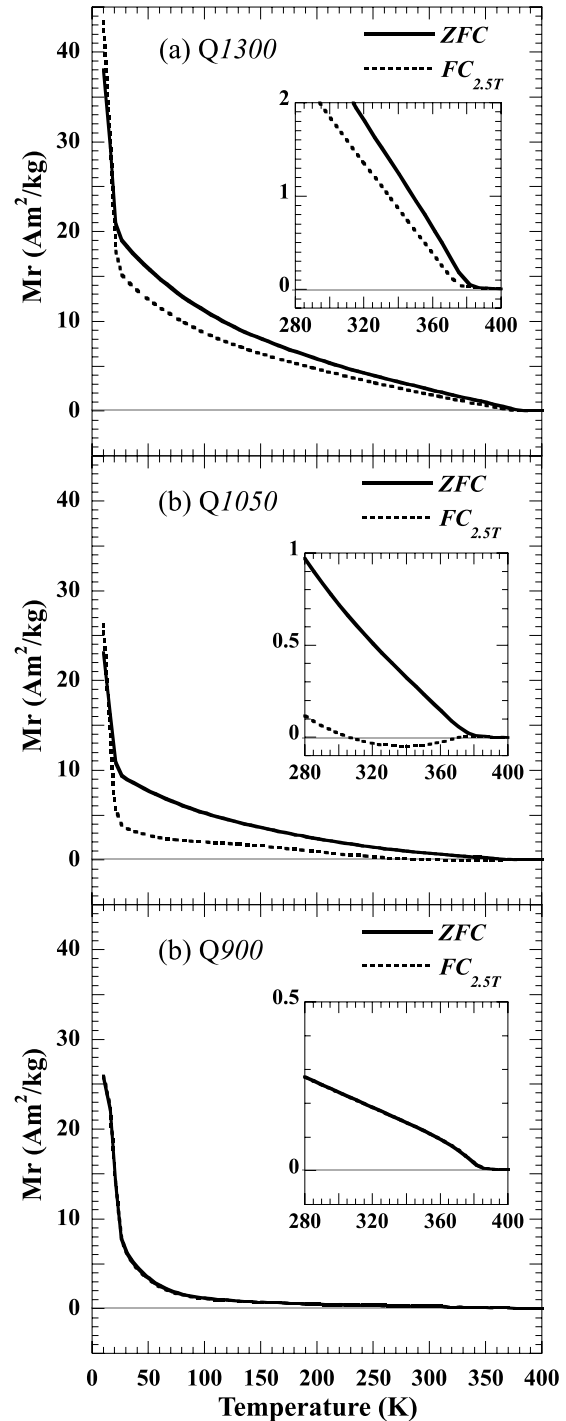


**Figure 5.** Low-temperature demagnetization of a saturation isothermal remanent magnetization (SIRM) acquired at 10 K in a magnetic field of 2.5 T following a ZFC (solid line) and a FC (dashed line) pretreatment.



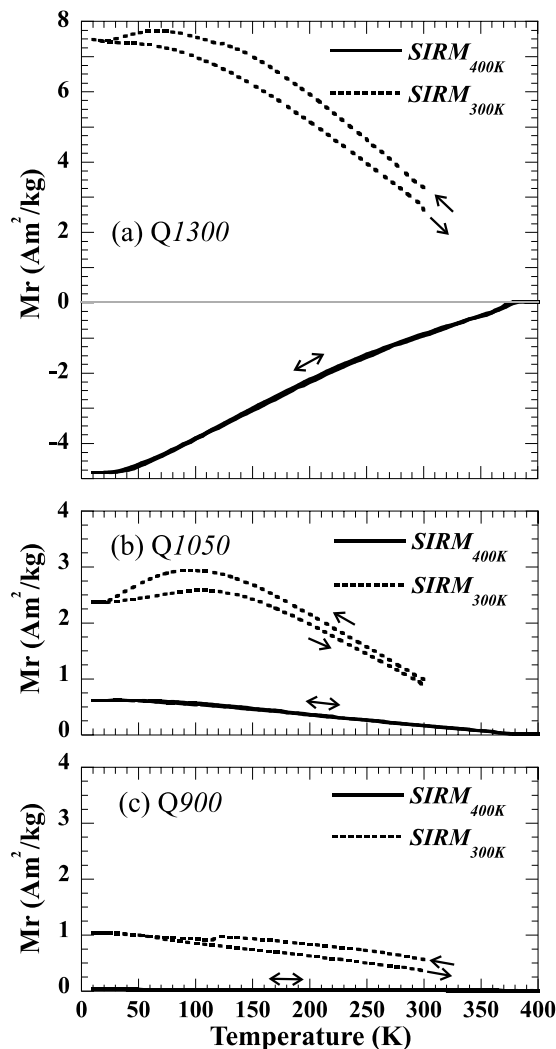


**Figure 6.** The temperature dependence of the saturation isothermal remanent magnetizations (SIRM) acquired at 400 K ( $SIRM_{400K}$ ) and 300 K ( $SIRM_{300K}$ ) in a 2.5 T magnetic field, measured by cycling the SIRMs to 10 K and back to their acquisition temperature.

### 5.1. ZFC and FC $SIRM_{10K}$

[17] Low temperature demagnetization of saturation isothermal remanent magnetizations acquired at 10 K ( $SIRM_{10K}$ ) in magnetic fields of 2.5 T following zero-field cooling (ZFC) or field cooling (FC) pretreatments were measured using the MPMS on all three specimens. The experiments were conducted over two temperature ranges, 10 K to 300 K (not shown) and 10 K to 400 K (Figure 5). The two temperature ranges permit us to evaluate the consequences of zero field cooling and field cooling across  $T_C$  ( $\sim 380\text{K}$ ) of the cation ordered domains. Sample Q900 displays a complete independence of both pretreatment conditions (i.e., ZFC and FC) (see Figure 5c) and whether field cooling began above (at 400 K) or below (at 300 K)  $T_C$  of the cation ordered domains. This is not the case for Q1300 and Q1050. Both of these samples display weaker FC remanence than ZFC remanence, above 20 K, when the samples are FC across  $T_C$  of the cation ordered domains

(Figures 5a and 5b). When field cooling begins at 300 K, FC remanence is slightly stronger than ZFC remanence (not shown). The inset plots in Figure 5 show that for all samples ZFC and FC remanence are equal above  $\sim 380$  K and nearly zero.

### 5.2. Cooling-Warming Cycles of $SIRM_{300K}$ and $SIRM_{400K}$

[18] The specimens were subjected to a 2.5 T magnetic field at 400 K or at 300 K (after being cooled from 400 K to 300 K in zero field) inducing an  $SIRM_{400K}$  and  $SIRM_{300K}$  respectively. In zero field the temperature dependence of the imparted remanence is measured by cycling to 10 K (cooling) before warming back to the temperature of acquisition. These experiments were also conducted using a MPMS. Results for all three specimens are plotted in Figure 6. All three  $SIRM_{300K}$  are positive (i.e., normal), increase as temperature decreases and exhibit slight irreversibility. Remanence magnitudes while cycling  $SIRM_{300K}$  are strongest in sample Q1300 and weakest in Q900. The same is true for  $SIRM_{400K}$  but unlike  $SIRM_{300K}$ ,  $SIRM_{400K}$  cooling and warming cycles display good reversibility. Absolute magnitudes increase with decreasing temperature but only below 380 K. Between 400 K (acquisition temperature) and 380 K, remanent magnetizations show little to no increase from the initial remanence acquired at 400 K (Q1300, 13.3  $\text{mAm}^2/\text{kg}$ ; Q1050, 15.8  $\text{mAm}^2/\text{kg}$ ; Q900, 6.4  $\text{mAm}^2/\text{kg}$ ). Lastly, a 2.5 T field applied at 400 K, some 20 K above  $T_C$  of the cation ordered domains, produces a RTRM in Q1300 but not in Q1050.

### 5.3. $M_{ZFC}$ and $M_{FC}$

[19] The following experiments enable us to calculate the remanent magnetization values across the temperature range of 10 K to 400 K from magnetizations induced in small DC fields following ZFC ( $M_{ZFC}$ ) or FC ( $M_{FC}$ ) pretreatments from 400 K to 10 K. The FC pretreatment utilized the same magnetic field strength as applied during the magnetization measurements. The remanent magnetization is calculated from the difference between  $M_{FC}$  response (induced + remanent magnetization) and  $M_{ZFC}$  response (induced magnetization). Plotted in Figures 7a–7c are the results for Q1300, Q900 and Q1050, respectively, subjected to DC fields of 5 mT, while Figure 7d displays the response of Q1050 to a 50 mT DC field.  $M_{ZFC}$  and  $M_{FC}$  curves measured in 5 mT are superimposed from 400 K to  $\sim 380$  K at which point the cation ordered domains magnetically order and acquire a normal TRM for Q1300 (Figure 7a) and Q900 (Figure 7b). In Q1050 (Figure 7c),  $M_{ZFC}$  and  $M_{FC}$  remain approximately superimposed until  $\sim 240$  K. Below this temperature Q1050 acquires a reversed TRM. In a 50 mT applied field (Figure 7d), Q1050 acquires a normal TRM at  $\sim 360$  K and above this temperature  $M_{ZFC}$  and  $M_{FC}$  curves are superimposed.

### 5.4. TRM

[20] The experiments in sections 5.1 through 5.3 were carried out on the MPMS where the maximum temperature achievable is 400 K. Therefore, by using the MPMS we can impart a TRM on the cation ordered domains ( $T_C \approx 380$  K) but we cannot impart a TRM on region 2 because its magnetic ordering temperature lies between 410 K and

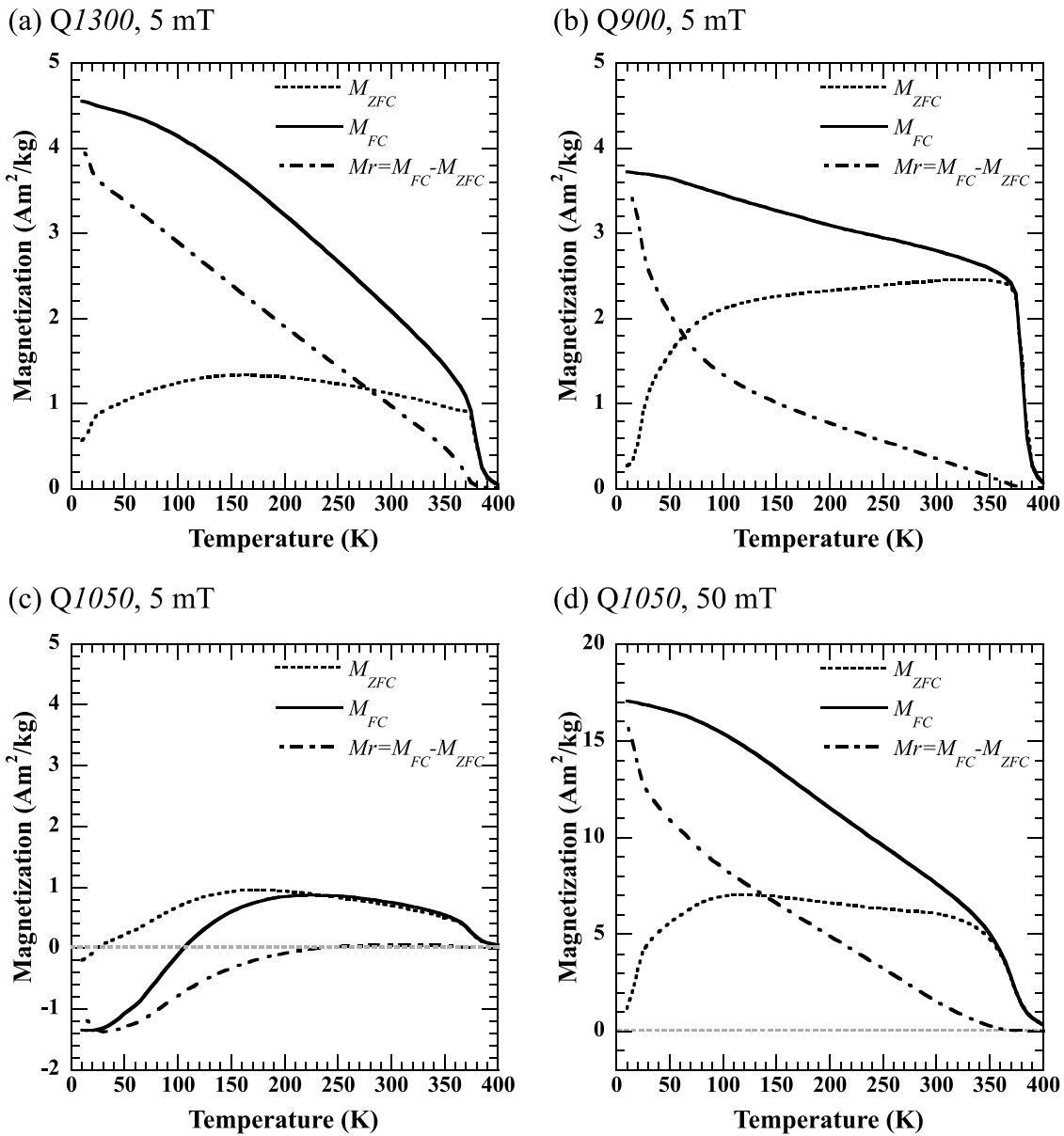


**Figure 7.** Remanent magnetization (dash-dotted line) calculated from low-field induced magnetization measured on warming from 10 K to 400 K following a ZFC (dashed line) or a FC (solid line) pretreatment from 400 K to 10 K. The inducing magnetic field strength is the same as the applied field during the FC pretreatment. Results for (a) Q1300, (b) Q900, and (c) Q1050 in a 5 mT inducing field. (d) Result of Q1050 in a 50 mT inducing field.

425 K, dependent on the sample (i.e., thermal history), based on results presented in section 3. The TRM experiments presented in this section were carried out on a VSM equipped with a flowing helium gas furnace which has a lower temperature limit of 300 K. The samples were first thermally demagnetized from 300 K to 573 K in zero field. The samples were then cooled from 573 K to 300 K imparting a TRM in variable magnetic field strengths. Plotted in Figure 8 are TRM imparted in 1 mT, 3 mT, 5 mT, and 7 mT for Q1300 (Figure 8a) and Q1050 (Figure 8c).

[21] In Q1300, TRM imparted in 1 mT, 3 mT and 5 mT are characterized by three components while the TRM imparted in 7 mT displays only two components. These are amplified by observing the first derivative of the TRM curves

(Figure 8b). The high-temperature component, above  $\sim 380$  K is normal and weak. The unblocking temperature of this component, presumably associated with region 2, is difficult to determine given the very weak remanence it acquires. In section 3, we had estimated a  $T_C$  of approximately 418 K. The second component observed in the 1 mT, 3 mT, and 5 mT TRM are all reversed and have unblocking temperatures of  $\sim 380$  K. As the imparting field increases, the intensity of the reversed component decreases and in a magnetic field of 7 mT the component is normal. The third component, unblocking at  $\sim 370$  K, is reversed for the 1 mT and 3 mT TRM but normal for the 5 mT TRM.

[22] In Q1050, within the allowable temperature range of this experiment, reversed TRM are observed in applied

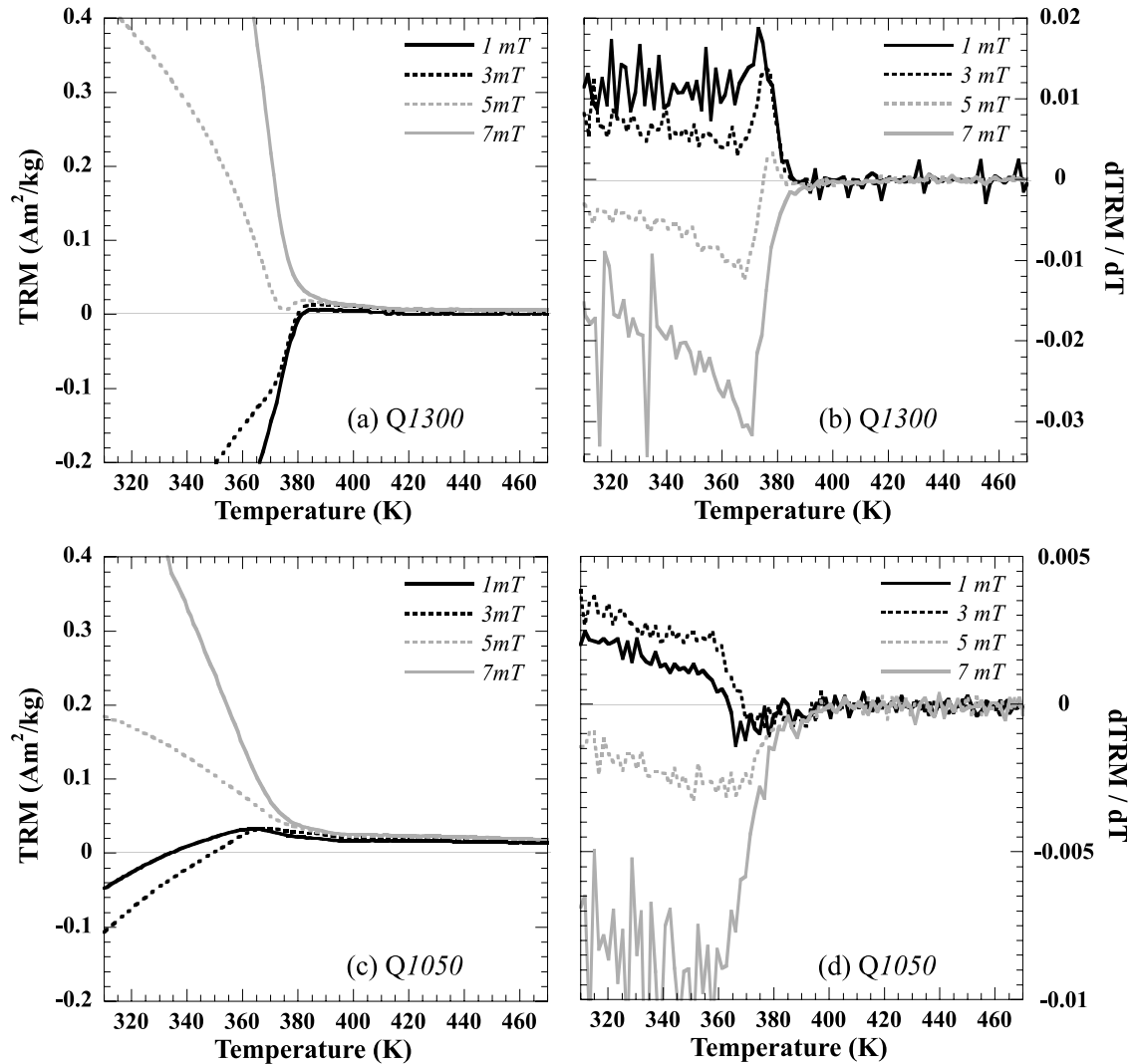


**Figure 8.** Thermoremanent magnetization imparted in magnetic fields of 1, 3, 5 and 7 mT in (a) Q1300 and (c) Q1050 and (b and d) the corresponding first derivatives, respectively. See text for further explanation.

magnetic fields of 1 mT and 3 mT and have unblocking temperatures of  $\sim 365$  K and  $\sim 370$  K respectively (see Figures 8c and 8d). While a RTRM in 5 mT is not observed in this experiment, results in section 5.3 indicate that a magnetic field of 5 mT produced a reversed remanence component at temperatures below 240 K. In all applied fields the remanence component unblocking at  $\sim 380$  K has a normal polarity. For TRM imparted in 1 mT and 3 mT, the normal components, located between the RTRM at lower temperature and the remanence component of the region 2 above  $\sim 380$  K, have very small intensities, approximately  $0.011 \text{ Am}^2/\text{kg}$  (TRM in 1 mT) and  $0.005 \text{ Am}^2/\text{kg}$  (TRM in 3 mT). The background remanence which persists beyond the final  $T_C$  estimated at  $\sim 410$  K (see section 3), results from the titanomagnetite contamination present in this sample (see section 2). We rule out the possibility of the TM phase influencing the acquisition of an RTRM in Q1050 based on the reasoning that exchange anisotropy between a spinel and a rhombohedral phase is less likely to occur (less favorable) than between two rhombohedral

phases. Our interpretations of the TRM observations in both samples will be discussed in the following section.

## 6. Discussion

[23] The synthetic ferrian ilmenite ( $y = 0.7$ ) specimens investigated were quenched either from a temperature superior to that of the cation order-disorder transition (see Figure 1) permitting, under favorable conditions, the acquisition of a reversed thermoremanent magnetization (RTRM) (i.e., Q1300 and Q1050) or from a temperature below that of the cation order-disorder transition where RTRM is never observed (i.e., Q900) in single-phase compositions. Prior work by Lawson *et al.* [1981] and Nord and Lawson [1989, 1992] on these same samples determined among other properties the relative abundance of cation ordered regions and cation disordered regions (see Table 1) and the spatial relationship between these regions from dark-field transmission electron microscopy. Their observations confirmed the model that cation ordered regions (ferrimagnetic) form

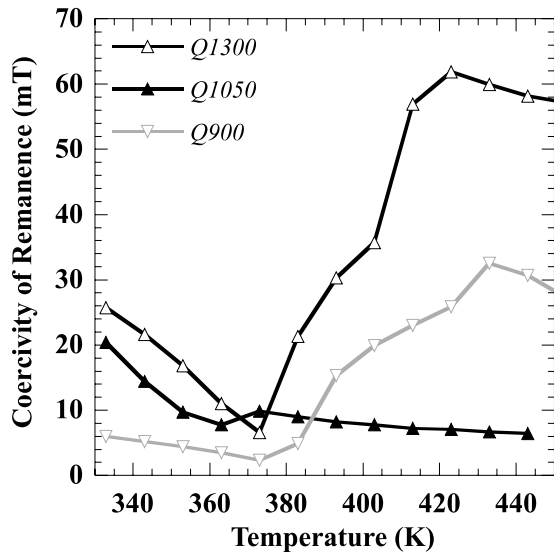


**Figure 9.** Temperature dependence of the coercivity of remanence across a temperature range straddling the magnetic ordering temperatures of the cation ordered domains ( $\sim 380$  K) and that of the cation disordered boundaries listed in Table 3. The raw data of the coercivity of remanence experiments are listed in Table 4.

(chemical) domains that are surrounded or enclosed within cation disordered (antiferromagnetic with parasitic moment) boundaries or matrix. The discussion which follows will concentrate on specimens Q1300 and Q1050 since our goal is to elucidate the mechanism of RTRM.

[24] The low-field AC magnetic susceptibility experiments (Figure 3) and especially the high-field induced remanence experiments (insets of Figure 5) provide compelling evidence that the cation ordered domains ferrimagnetically order at  $\sim 380$  K and that the magnetic ordering temperature is independent of thermal history. However, as previously determined by others, the grain size of the cation ordered domains is not independent of thermal history (see Table 1). The lack of any break in slope near 380 K in the  $M_S(T)$  data (Figures 2a through 2c) suggest that the mag-

netocrystalline anisotropy energy of the cation ordered domains is lower than that of the cation disordered boundaries. The temperature dependence of the coercivity of remanence plotted in Figure 9 (raw data are listed in Table 4) also points to stronger anisotropy energy in the cation disordered boundaries than in the cation ordered domains. The magnetic ordering temperature of the cation ordered domains is 380 K and is independent of thermal history. Therefore the magnetic ordering transition to paramagnetism observed at 418 K (Q1300), at 410 K (Q1050) and at 425 K (Q900) belong to the antiferromagnetic cation disordered boundaries. This is further supported by the extremely low remanence and induced magnetizations measured above 380 K (see, for example, Figure 5). Overall, our data appear to support unambiguously the common view of models proposed by Uyeda [1958], Hoffman [1975], and Nord and Lawson [1992] in that RTRM results from the direct interaction of ferrimagnetic cation ordered domains with antiferromagnetic cation disordered domains. Therefore region 2 is antiferromagnetic.

[25] The ZFC and FC hysteresis loop experiments presented in section 4 predict that the effective exchange anisotropy enabling the acquisition of RTRM has a strength of  $\sim 2.7$  mT and 12 mT in Q1300 and Q1050, respectively. Therefore we should expect that applied magnetic fields much stronger than that of the exchange anisotropy would align the ferrimagnetic moments of the cation ordered domains parallel to the applied field resulting in a normal TRM. Remanent magnetizations calculated from  $M_{ZFC}$  and  $M_{FC}$  measurements (Figure 7) appear to corroborate this. A DC field of 5 mT does not permit Q1300 to develop a RTRM while it does for Q1050. However, for Q1050 the TRM intensity only becomes negative below 240 K even though the cation ordered domains magnetically ordered at 380 K. No RTRM is produced in Q1050 in a DC field of 50 mT. A field of 50 mT is much stronger than that of the effective exchange anisotropy, 12 mT (see section 4), and the bulk coercivity (see Table 2). A strong magnetic field applied 20 K above  $T_C$  (380 K) of the cation ordered domains but below the magnetic ordering temperature of the cation disordered boundary followed by zero-field cooling across  $T_C$  of the cation ordered domains produces a

**Table 4.** Raw Data of the Experiment Measuring the Temperature Dependence of the Coercivity of Remanence ( $B_{CR}$ ) From the DC Demagnetization of the Saturation Isothermal Remanent Magnetization (SIRM) Plotted in Figure 9<sup>a</sup>

Temperature, K	Q1050		Q1300		Q900	
	SIRM, $\text{Am}^2/\text{kg}$	$B_{CR}$ , mT	SIRM, $\text{Am}^2/\text{kg}$	$B_{CR}$ , mT	SIRM, $\text{Am}^2/\text{kg}$	$B_{CR}$ , mT
333	$0.704 \pm 0.003$	20.4	$2.483 \pm 0.012$	25.7	$0.543 \pm 0.003$	6.0
343	$0.472 \pm 0.002$	14.4	$1.976 \pm 0.009$	21.6	$0.467 \pm 0.003$	5.2
353	$0.312 \pm 0.001$	9.7	$1.436 \pm 0.007$	16.8	$0.385 \pm 0.002$	4.4
363	$0.164 \pm 0.001$	7.7	$0.848 \pm 0.004$	11.0	$0.292 \pm 0.002$	3.5
373	$0.066 \pm 0.000$	9.8	$0.280 \pm 0.001$	6.6	$0.167 \pm 0.001$	2.4
383	$0.043 \pm 0.000$	9.0	$0.039 \pm 0.000$	21.3	$0.026 \pm 0.000$	4.9
393	$0.035 \pm 0.000$	8.2	$0.019 \pm 0.000$	30.3	$0.010 \pm 0.000$	15.3
403	$0.032 \pm 0.000$	7.8	$0.013 \pm 0.000$	35.7	$0.006 \pm 0.000$	19.9
413	$0.029 \pm 0.000$	7.2	$0.008 \pm 0.000$	56.9	$0.005 \pm 0.000$	23.0
423	$0.029 \pm 0.000$	7.0	$0.007 \pm 0.000$	61.9	$0.003 \pm 0.000$	25.9
433	$0.027 \pm 0.000$	6.6	$0.006 \pm 0.000$	59.9	$0.004 \pm 0.000$	32.5
443	$0.025 \pm 0.000$	6.5	$0.006 \pm 0.000$	58.2	$0.002 \pm 0.000$	30.7
453	-	-	$0.006 \pm 0.000$	57.2	$0.002 \pm 0.000$	27.2

<sup>a</sup>Because of the mounting process the mass of the samples measured on the high-temperature VSM is unknown but was calculated from the 100 K temperature overlap of the high- and low-temperature  $M_{[1,5T]}$  data (see Figures 2a–2c), where the mass of samples for the low-temperature measurements is known. The calculated masses and their standard deviations are listed in Table 3 and were used here to mass normalize the SIRM data.

RTRM in Q1300 but not in Q1050 (Figure 6). Results in Figure 5 show that cooling across  $T_C$  of the cation ordered domains in a 2.5 T magnetic field also produces a RTRM, which we deduce from the observation that FC remanences are weaker than ZFC remanences. Since the net remanence intensities remain positive, we conclude that only certain cation ordered domains are able to acquire a reversed remanent magnetization component. Furthermore, as temperatures decrease, the intensity of the reversed remanence component increases more rapidly than the normal remanence component.

[26] The above key observations along with results in Figure 8 indicate that perhaps the size of the cation ordered domains play a role in the acquisition of RTRM. The cation ordered domains in Q1300 are characterized as having an average size of  $\sim 71$  nm [Nord and Lawson, 1992] (see Table 1) and appear to promote the acquisition of RTRM while cation ordered domains in Q1050 are characterized as having an average size of  $\sim 37$  nm [Nord and Lawson, 1992] (see Table 1) and appear to inhibit the acquisition of RTRM.

[27] The observations from Q1050 can be adequately explained if one considers that its cation ordered domains have a superparamagnetic (SP) behavior just below their  $T_C$ . Low coercivities (Table 2) and coercivities of remanence (Figure 9) immediately below 380 K support an SP nature of the cation ordered domains in Q1050. Perhaps even more convincing is the frequency dependence of the in-phase magnetic susceptibility of Q1050 below 380 K (Figure 3c) compared to that of Q1300 (Figure 3b). Note that the cation disordered boundaries do not behave superparamagnetically, suggested by the increased in coercivity of remanence above 380 K (Figure 9) even though their sizes are smaller than that of the cation ordered domains. This is due to the low saturation magnetization of the cation disordered boundaries which effectively suppresses the critical size of the superparamagnetic to stable single domain threshold. The limited increase in  $B_{CR}$  observed in Q1050 in comparison to Q1300 and Q900 may be an expression of the TM phase present in Q1050 (see section 2).

[28] Thermal activation energy, destabilizing the magnetic moments of cation ordered domains, works against the exchange anisotropy and results in the acquisition of a RTRM at 380 K being inhibited. As the temperature decreases thermal activation energy decreases, cation ordered domains stabilize (block) and a RTRM is able to develop. The strength of the applied field also plays a role. Clearly cooling through 380 K in zero field cannot produce a RTRM at any temperature even if a strong magnetic field is applied just above  $T_C$  (Figure 6b). However, Figure 8c shows that in 1 mT a reversed component is initiated at  $\sim 365$  K and a negative TRM intensity results by 330 K. Better yet, in 3 mT, a RTRM component is initiated at  $\sim 370$  K and a negative TRM intensity results by 350 K. However in 5 mT a negative TRM intensity appears at 240 K (Figure 7c) and as the applied magnetic field increases the temperature at which RTRM is initiated decreases until no RTRM is produced presumably above 12 mT, the measured effective exchange anisotropy. It seems that for Q1050, DC fields weaker than 3 mT aid the exchange anisotropy in overcoming the thermal activation energy randomizing the cation ordered domain's magnetic moments. Applied fields approaching 3 mT but less than 3 mT

are most efficient in enabling the acquisition of a RTRM. However, fields stronger than 3 mT begin to bias the magnetic moments of some cation ordered regions parallel to the external applied field at higher temperatures. Consequently, TRM intensities are positive immediately below 380 K but as temperatures decrease cation ordered domains begin to block in a stable magnetic state antiparallel to the external field. Consequently, this leads to an eventual net TRM with a negative intensity.

[29] In contrast, the efficiency of sample Q1300 in acquiring a RTRM, even though the effective exchange anisotropy has a magnetic field strength of only  $\sim 2.7$  mT, is due to the larger size of the cation ordered domains. The TRM experiments plotted in Figure 8a suggest a magnetic zoning within the cation ordered domains. This magnetic zoning is most apparent in the TRM data imparted in a 5 mT external field. A 5 mT external field is larger than the exchange anisotropy field strength but a reversed TRM component is acquired and unblocks at 380 K even though the TRM intensity never becomes negative. The dominant normal TRM unblocks at  $\sim 370$  K. An external applied field of 3 mT, approximately equal to the exchange anisotropy, produces a RTRM immediately below 380 K but a change in slope occurs at  $\sim 370$  K. It appears that the exchange anisotropy is able to exchange couple across the entire cation ordered domain when external magnetic field strength are much lower than its own magnetic field strength. As the external applied field approaches that of the exchange anisotropy, the cation ordered region furthest from cation disordered boundaries begin to align its magnetic moments parallel to the external applied field. Note that it is not necessary to have a differential Fe content within the cation ordered domains in order to develop a magnetic zoning. The short-lived RTRM component observed in the 5 mT TRM run (Figure 8a) results from a very short range penetration of exchange coupling within the cation ordered domains. An external magnetic field of 7 mT does not permit any magnetic moments to be coupled by exchange anisotropy antiparallel to the magnetic field.

[30] Our investigation and interpretations benefited from the use of previously well characterized synthetic ferrian ilmenite. It is our opinion, such studies on synthetic samples are necessary in order to understand behaviors in natural samples often complicated by multicomponent mineralogy. The results presented herein, in particular the TRM behavior observed when cation ordered domains are superparamagnetic may provide an alternative explanation for the behavior observed in natural ferrian ilmenite ( $y = 0.50-0.52$ ) of the 1991 Mt. Pinatubo eruption reported by Prévot *et al.* [2001] (see their Figure 3). They refer to cation ordered domains as "ordered nanodomain" acknowledging their small size. Furthermore, they conclude that the RTRM results for the exchange interaction between the ferrimagnetic rim and ferrimagnetic core of the "ordered nanodomains" based on the observation of a normal remanence component of a magnitude of 0.25 A/m (extrapolated to room temperature) persisting at a higher temperature than the RTRM. This observation is analogous to our observations in sample Q1050 (Figure 8c) but we have also demonstrated that this sample may, in favorable conditions, acquire a RTRM immediately below  $T_C$  of the cation ordered domains (inset of Figure 5b). Consequently, RTRM

cannot result from a ferrimagnetic – ferrimagnetic exchange interaction.

## 7. Conclusion

[31] The careful remanence and induced magnetization experiments conducted on synthetic single-phase ferrian ilmenite ( $y = 0.7$ ) presented herein, lead us to conclude the following.

[32] 1. RTRM results from exchange anisotropy when, under favorable conditions, a direct exchange interaction between ferrimagnetic cation ordered domains and antiferromagnetic cation disordered boundaries (possessing a weak parasitic moment) is manifested in ferrian ilmenite phases quenched at a temperature greater than that of the cation order-disorder transition. This is in agreement with the common points of models proposed by Hoffman [1975], Nord and Lawson [1992], and Uyeda [1958].

[33] 2. Favorable conditions for the acquisition of RTRM are controlled by the size of the cation ordered domains, the strength of the exchange anisotropy and the strength of the external applied field.

[34] 3. The strength of the exchange anisotropy appears to increase as the ratio of cation disordered regions to cation ordered regions increases. Another consequence of increasing cation disordered region to cation ordered region ratio is the greater abundance of smaller magnetically unstable cation ordered domains. These appear to inhibit the acquisition of RTRM immediately below their  $T_C$  due to thermal activation energy and an as yet unclear competition between the exchange anisotropy and the external applied field.

[35] 4. For a given bulk composition, the magnetic ordering temperature of the ferrimagnetic cation ordered domains is independent of thermal history (i.e., quenching temperature).

[36] **Acknowledgments.** We would like to thank C.A. Lawson and G.L. Nord for the synthetic samples. The manuscript was reviewed by R. T. Merrill, S. McEnroe and associate editor L. Tauxe. This research benefited from the award of the Stanwood Johnston Memorial Fellowship to F. Lagroix. This is contribution #0404 of the Institute for Rock Magnetism, which is funded by the W. M. Keck Foundation, the Earth Sciences Division of the National Science Foundation and the University of Minnesota.

## References

- Ade-Hall, J. M., R. L. Wilson, and P. J. Smith (1965), The petrology, Curie points and natural magnetization of basic lavas, *Geophys. J.*, *9*, 323–336.
- Bina, M., J. C. Tanguy, V. Hoffmann, M. Prévot, E. L. Listanco, R. Keller, K. T. Fehr, A. Goguitchaichvili, and R. S. Punongbayan (1999), A detailed magnetic and mineralogical study of self-reversed dacitic pumices from the 1991 Pinatubo eruption (Philippines), *Geophys. J. Int.*, *138*, 159–178.
- Carmichael, C. M. (1961), The magnetic properties of ilmenite-hematite crystals, *Proc. R. Soc. London, Ser. A*, *263*, 508–530.
- Ghiorso, M. S. (1997), Thermodynamic analysis of the effect of magnetic ordering on miscibility gaps in the FeTi cubic and rhombohedral oxide minerals and the FeTi oxide geothermometer, *Phys. Chem. Miner.*, *25*, 28–38.
- Goguitchaichvili, A., and M. Prévot (2000), Magnetism of oriented single crystals of hemoilmenite with self-reversed thermoremanent magnetization, *J. Geophys. Res.*, *105*(B2), 2761–2780.
- Grommé, G. S., T. L. Wright, and D. L. Peck (1969), Magnetic properties and oxidation of iron-titanium oxide minerals in Alae and Makaopuhi lava lakes, *J. Geophys. Res.*, *74*, 5277–5294.
- Hoffman, K. A. (1975), Cation diffusion processes and self-reversal of thermoremanent magnetization in the ilmenite-hematite solid solution series, *Geophys. J. R. Astron. Soc.*, *41*, 65–80.
- Ishikawa, Y. (1958), An order-disorder transformation phenomenon in the  $\text{FeTiO}_3\text{-Fe}_2\text{O}_3$  solid solution series, *J. Phys. Soc. Jpn.*, *13*(8), 828–837.
- Ishikawa, Y., and S. Akimoto (1957), Magnetic properties of the  $\text{FeTiO}_3\text{-Fe}_2\text{O}_3$  solid solution series, *J. Phys. Soc. Jpn.*, *12*(10), 1083–1098.
- Ishikawa, Y., and Y. Syono (1963), Order-disorder transformation and reverse thermo-remanent magnetism in the  $\text{FeTiO}_3\text{-Fe}_2\text{O}_3$  system, *J. Phys. Chem. Solids*, *24*, 517–528.
- Ishikawa, Y., N. Saito, M. Arai, Y. Watanabe, and H. Takei (1985), A new oxide spin glass system of  $(1-x)\text{FeTiO}_3\text{-}x\text{Fe}_2\text{O}_3$ . I. Magnetic properties, *J. Phys. Soc. Jpn.*, *54*(1), 312–325.
- Lagroix, F., S. K. Banerjee, and M. Jackson (2004), Magnetic properties of the Old Crow tephra: Identification of a complex iron titanium oxide mineralogy, *J. Geophys. Res.*, *109*, B01104, doi:10.1029/2003JB002678.
- Lawson, C. A. (1981), Magnetic and microstructural properties of minerals of the ilmenite-hematite solid solution series with special reference to the phenomenon of reverse thermoremanent magnetism, Ph.D. thesis, Princeton Univ., Princeton, N. J.
- Lawson, C. A., G. L. Nord, E. Dowty, and R. B. Hargraves (1981), Anti-phase domains and reverse thermoremanent magnetism in ilmenite-hematite minerals, *Science*, *213*, 1372–1374.
- Meiklejohn, W. H. (1962), Exchange anisotropy—A review, *J. Appl. Phys.*, *33*(3), 1328–1335.
- Meiklejohn, W. H., and C. P. Bean (1957), New magnetic anisotropy, *Phys. Rev.*, *105*(3), 904–913.
- Meiklejohn, W. H., and R. E. Carter (1959), Exchange anisotropy in rock magnetism, *J. Appl. Phys.*, *30*(2), 2020.
- Meiklejohn, W. H., and R. E. Carter (1960), Exchange anisotropy in rock magnetism, *J. Appl. Phys.*, *31*(5), 164S–165S.
- Merrill, R. T., and G. S. Grommé (1967), Non-reproducible self-reversal of magnetization in diorite, *J. Geophys. Res.*, *74*, 2014–2024.
- Moskowitz, B. M. (1981), Methods for estimating Curie temperatures of titanomagnetites from experimental  $J_s$ -data, *Earth Planet. Sci. Lett.*, *53*, 84–88.
- Nagata, T., and S. Akimoto (1956), Magnetic properties of ferromagnetic ilmenites, *Pure Appl. Geophys.*, *34*, 36–50.
- Nagata, T., S. Akimoto, and S. Uyeda (1951), Reverse thermo-remanent magnetism, *Proc. Jpn. Acad.*, *27*(10), 643–645.
- Nagata, T., S. Akimoto, and S. Uyeda (1953), Self-reversal of thermoremanent magnetism of igneous rocks (III), *J. Geomagn. Geoelectr.*, *5*(4), 168–184.
- Nord, G. L., and C. A. Lawson (1989), Order-disorder transition-induced twin boundaries and magnetic properties in ilmenite-hematite, *Am. Mineral.*, *74*, 160–176.
- Nord, G. L., and C. A. Lawson (1992), Magnetic properties of ilmenite<sub>70</sub>hematite<sub>30</sub>: Effects of transformation-induced twin boundaries, *J. Geophys. Res.*, *97*, 10,897–10,910.
- Prévot, M., K. A. Hoffman, A. Goguitchaichvili, J.-C. Doukhan, V. Schcherbakov, and M. Bina (2001), The mechanism of self-reversal of thermoremanence in natural hemoilmenite crystals: New experimental data and model, *Phys. Earth Planet. Inter.*, *126*, 75–92.
- Tauxe, L. (1998), *Paleomagnetic Principles and Practice*, 312 pp., Springer, New York.
- Uyeda, S. (1955), Magnetic interaction between ferromagnetic materials contained in rocks, *J. Geomagn. Geoelectr.*, *7*(1–2), 9–36.
- Uyeda, S. (1957), Thermo-remanent magnetism and coercive force of the ilmenite-hematite series, *J. Geomagn. Geoelectr.*, *9*(2), 61–78.
- Uyeda, S. (1958), Thermo-remanent magnetization as a medium of paleomagnetism, with special reference to reverse thermo-remanent magnetism, *Jpn. J. Geophys.*, *2*, 123 pp.
- Westcott-Lewis, M. F., and L. G. Parry (1971), Thermoremanence in synthetic rhombohedral iron-titanium oxides, *Aust. J. Phys.*, *24*, 735–742.

S. K. Banerjee and B. M. Moskowitz, Department of Geology and Geophysics, University of Minnesota, Minneapolis, MN 55455, USA.

F. Lagroix, IGP-CNRS, Laboratoire de Paléomagnétisme, F-75252 Paris Cedex 05, France. (lagroix@ipgg.jussieu.fr)